

Anisotropic Magnification Distortion of the 3D Galaxy Correlation: I. Real Space

Lam Hui^{1,2}, Enrique Gaztañaga³ and Marilena LoVerde^{1,2}

¹*Institute for Strings, Cosmology and Astroparticle Physics (ISCAP)*

²*Department of Physics, Columbia University, New York, NY 10027*

³*Institut de Ciències de l'Espai, IEEC-CSIC, Campus UAB,*

F. de Ciències, Torre C5 par-2, Barcelona 08193, Spain

lhui@astro.columbia.edu, gazta@ieec.uab.es, marilena@phys.columbia.edu

(Dated: October 22, 2018)

It has long been known that gravitational lensing, primarily via magnification bias, modifies the observed galaxy (or quasar) clustering. Such discussions have largely focused on the 2D angular correlation function. Here and in a companion paper (Paper II) we explore how magnification bias distorts the 3D correlation function and power spectrum, as first considered by Matsubara (2000). The interesting point is: the distortion is anisotropic. Magnification bias in general preferentially enhances the observed correlation in the line-of-sight (LOS) orientation, especially on large scales. For instance, at a LOS separation of ~ 100 Mpc/h, where the intrinsic galaxy-galaxy correlation is rather weak, the observed correlation can be enhanced by lensing by a factor of a few, even at a modest redshift of $z \sim 0.35$. This effect presents an interesting opportunity as well as challenge. The opportunity: this lensing anisotropy is distinctive, making it possible to separately measure the galaxy-galaxy, galaxy-magnification *and* magnification-magnification correlations, without measuring galaxy shapes. The anisotropy is distinguishable from the well known distortion due to peculiar motions, as will be discussed in Paper II. The challenge: the magnification distortion of the galaxy correlation must be accounted for in interpreting data as precision improves. For instance, the ~ 100 Mpc/h baryon acoustic oscillation scale in the correlation function is shifted by up to $\sim 3\%$ in the LOS orientation, and up to $\sim 0.6\%$ in the monopole, depending on the galaxy bias, redshift and number count slope. The corresponding shifts in the inferred Hubble parameter and angular diameter distance, if ignored, could significantly bias measurements of the dark energy equation of state. Lastly, magnification distortion offers a plausible explanation for the well known excess correlations seen in pencil beam surveys.

PACS numbers: 98.80.-k; 98.80.Es; 98.65.Dx; 95.35.+d

I. INTRODUCTION

Since the pioneering work of [1], it has been appreciated that gravitational lensing modifies the spatial distribution of high redshift objects, such as galaxies or quasars (henceforth, the term ‘galaxies’ can be viewed as synonymous with quasars or any sample of survey objects). Suppose for instance there is a large mass concentration between some galaxies and the observer. The observed number density of galaxies would decrease due to the stretching of the apparent inter-galaxy spacing, but would increase due to the enhanced ability to see very faint galaxies that otherwise would have gone undetected. The size of the net effect depends on the number count slope. This effect is known as magnification bias.

The implications of this effect for the observed galaxy angular correlation function were worked out in [2, 3, 4, 5]. It was pointed out by [6] that the magnification bias correction can be isolated by measuring the angular cross-correlation between galaxies at widely separated redshifts. This idea was subsequently realized in measurements by [7, 8] through the cross-correlation of quasars and galaxies. See [9, 10, 11] for some recent theoretical work and references therein for earlier discussions of quasar-galaxy associations. See also [12] on the early use of magnification bias to make mass maps of galaxy

clusters.

With the important exception of Matsubara (2000) [13] (to which we will return at the end of this section), earlier papers have focused on the 2D angular correlation function. Here and in Paper II [14] of this series, we study the effect of magnification bias on the 3D correlation function and power spectrum. It is not hard to convince oneself that lensing makes the 3D correlation anisotropic. There are several effects at work, but the simplest one to think about is the following. Correlation function is measured by pair counts of galaxies. A pair of galaxies that are aligned along the line-of-sight (LOS) behave differently from a pair oriented transverse to the LOS. In the former case, the closer galaxy can lens the background one. The same does not happen in the transverse orientation. The net effect is an anisotropic observed correlation. One might think such an effect must be small: after all, typical LOS separations in clustering measurements are much smaller than the depth of surveys i.e. the lens is located much closer to the source than to the observer. However, one must remember that the lensing effect *grows* with the LOS separation, whereas the intrinsic galaxy correlation generally *drops* with separation. At a sufficiently large LOS separation, e.g. ~ 100 Mpc/h, where the intrinsic galaxy correlation is rather weak, one should not be too surprised that the lensing induced correlation can actu-

ally dominate. As we will show, the magnification bias induced anisotropy has a distinctive shape:

$$\xi_{\text{obs}}(\delta\chi, \delta x_{\perp}) = \xi_{gg}(\sqrt{\delta\chi^2 + \delta x_{\perp}^2}) + f(\delta x_{\perp})\delta\chi + g(\delta x_{\perp}) \quad (1)$$

where $\delta\chi$ and δx_{\perp} are the LOS and transverse separations respectively, ξ_{obs} is the observed correlation, ξ_{gg} is the intrinsic galaxy-galaxy correlation, $f\delta\chi$ is the galaxy-magnification correlation and g is the magnification-magnification correlation. Note that f and g are functions of the transverse separation only.

This distinctive anisotropy pattern makes it in principle possible to completely separate the three different contributions from data: galaxy-galaxy, galaxy-magnification and magnification-magnification correlations. (We will discuss other sources of anisotropy, such as peculiar motions in Paper II.) In a sense, the earlier work [6, 7, 8, 9, 10, 11] on angular correlation function for galaxies (or galaxies and quasars) at widely separated redshifts focused on one particular limit: a very large LOS separation $\delta\chi$ such that the galaxy-magnification correlation $f\delta\chi$ dominates. Studying more moderate LOS separations allows one to measure the magnification-magnification correlation g , which is perhaps of more theoretical interest since it relates directly to the mass. The key is to use the full 3D information, i.e. exploit the distinct dependence on $\delta\chi$ and δx_{\perp} of each term in eq. (1) to separately determine all three correlations.

Another important implication of eq. (1) is that care must be taken in interpreting galaxy clustering data. For instance, future galaxy surveys hope to determine the baryon oscillation scale to high precision [15, 16, 17, 18, 19, 20, 21]. Lensing induced shifts of the apparent baryon oscillation scale in the LOS direction affects the inference on the Hubble parameter $H(z)$, while shifts in the transverse direction affects the inference on the angular diameter distance. Recall that at a redshift of 1, a $\sim 1\%$ shift in angular diameter distance, or a $\sim 1\%$ shift in the Hubble parameter, corresponds to a $\sim 5\%$ shift in the dark energy equation of state. This means that even small lensing corrections are in principle a worry, not to mention potentially large corrections at high redshifts or at particularly susceptible orientations, such as the LOS direction.

The rest of the paper is organized as follows. In §II, we derive and numerically compute the magnification bias distortion, magnification distortion in short, of the observed galaxy clustering – §II A focuses on the overall anisotropy of the correlation function while §II B focuses on the baryon acoustic oscillations. In §III we present useful order of magnitude estimates which offer deeper insights into the numerical results of §II. We conclude in §IV, with a discussion of longstanding puzzles posed by pencil beam surveys. Appendix A contains a discussion of lensing corrections to the observed correlation other than those due to magnification bias, and a generaliza-

tion of the magnification bias effect to account for more complicated galaxy selection. Appendix B contains a discussion of the higher order Taylor expansion terms that are ignored in §II A.

In this paper, we focus exclusively on the effects of magnification distortion in configuration/real space. Paper II of this series explores this effect in Fourier space. Redshift space distortion due to peculiar motion and the Alcock-Paczynski effect will be discussed there as well. In yet another paper, we study the effects of magnification bias on the angular galaxy correlation function, focusing on the impacts on features of the power spectrum [22].

As this paper was being completed, two preprints appeared which discussed some related issues. Vallinotto et al. [23] explored the impact of lensing, especially magnification bias, on baryon oscillation measurements. They focused on the 2 point correlation function where the 2 points are at exactly the same redshift. They did not examine the full 3D correlation, in particular its anisotropy. Their findings are consistent with ours for pair separations oriented transverse to the LOS, and are more connected to our other paper on the angular correlation function [22]. Wagner et al. [24] examined the anisotropy of the 3D correlation that is introduced by light cone effects.

After this paper was initially circulated as a preprint, a pioneering paper by Matsubara (2000) [13] was kindly brought to our attention, where he derived an expression for 3D correlation function in the presence of magnification bias as well as redshift and cosmological distortions. In this paper, we have extended his analysis in a number of ways. By showing the 3D correlation function in terms of the LOS and transverse comoving separations (as opposed to redshift and angular separations as in [13]), the anisotropy pattern is brought out explicitly. We also emphasize the possibility to completely separate the three different contributions to the observed correlation function (see Fig. 2 below). As an application, we show how magnification distortion impacts baryon acoustic oscillation measurements. In Paper II, we also study the appearance of magnification distortion in Fourier space (as well as redshift space), which turns out to have some important and interesting qualitative differences from the appearance in configuration/real space.

II. MAGNIFICATION DISTORTION

Magnification bias introduces a well-known correction to the observed galaxy overdensity [1, 2, 3, 4, 6]:

$$\delta_{\text{obs}} = \delta_g + \delta_{\mu} \quad (2)$$

where the observed galaxy overdensity δ_{obs} , the original/intrinsic galaxy overdensity δ_g and the magnification bias correction δ_{μ} are all functions of the galaxy position, specified by the radial comoving distance χ and the angular position θ . The magnification bias correction is given by

$$\delta_{\mu} = (5s - 2)\kappa \quad (3)$$

where κ is the lensing convergence:

$$\kappa(\chi, \boldsymbol{\theta}) = \int_0^\chi d\chi' \frac{\chi'(\chi - \chi')}{\chi} \nabla_\perp^2 \phi(\chi', \boldsymbol{\theta}) \quad (4)$$

where ϕ is the gravitational potential, and ∇_\perp^2 is the 2D Laplacian in the transverse directions. We assume a flat universe – generalization to an open or a closed universe is straightforward. The symbol s stands for

$$s = \frac{d \log_{10} N(< m)}{dm} \quad (5)$$

where $N(< m)$ is the cumulative number counts for galaxies brighter than magnitude m . This assumes the galaxy sample is defined by a sharp faint-end cut-off. A broader definition of s for a more general galaxy selection is given in Appendix A.

Defining the galaxy bias b by $\delta_g = b\delta$, where δ is the mass overdensity, eq. (2) can be rewritten as

$$\frac{\delta_{\text{obs}}}{b} = \delta + \frac{5s - 2}{b} \kappa \quad (6)$$

The relative importance of the intrinsic clustering and the magnification bias correction is therefore controlled by, among other things, the sample dependent ratio $(5s - 2)/b$. The observed redshift-dependent luminosity function [25] can be used together with the halo model to estimate this ratio (see [26] for details). Fig. 1 shows this as a function of redshift for five different samples, each defined by a different B-band apparent magnitude cut-off. This figure should be viewed as an illustration of the range of possibilities only. The precise values of s and b depend sensitively on details of how the galaxy/quasar sample is selected, for instance subject to color cuts and so on. Unless otherwise stated, we adopt throughout this paper the value $(5s - 2)/b = 1$ to illustrate the effect of magnification bias on clustering measurements. For the correlation function or power spectrum, one can roughly scale the magnification bias correction we obtain by $(5s - 2)/b$ for galaxy redshift $\lesssim 1.5$ and by $(5s - 2)^2/b^2$ for redshift $\gtrsim 1.5$ (the former is dominated by the galaxy-magnification cross-term while the latter is dominated by the magnification-magnification term; see §II A). Note also that we assume a scale independent (linear) galaxy bias b . Nonlinear galaxy bias, as we will see, is important in certain situations including, surprisingly, some where large scale clustering measurements are involved (§II A).

The reader might wonder whether there are other lensing corrections to the observed galaxy overdensity. Indeed there are, and they are discussed further in Appendix A. It suffices to say magnification bias is the dominant effect for regimes of practical interest.

In all illustrative examples below, we employ the following cosmological parameters: the Hubble constant $h = 0.7$, matter density $\Omega_m = 0.27$, cosmological constant $\Omega_\Lambda = 0.73$, baryon density $\Omega_b = 0.046$, power spectrum slope $n = 0.95$ and normalization $\sigma_8 = 0.8$. We employ the transfer function of [27], and the prescription of [28] for the nonlinear power spectrum.

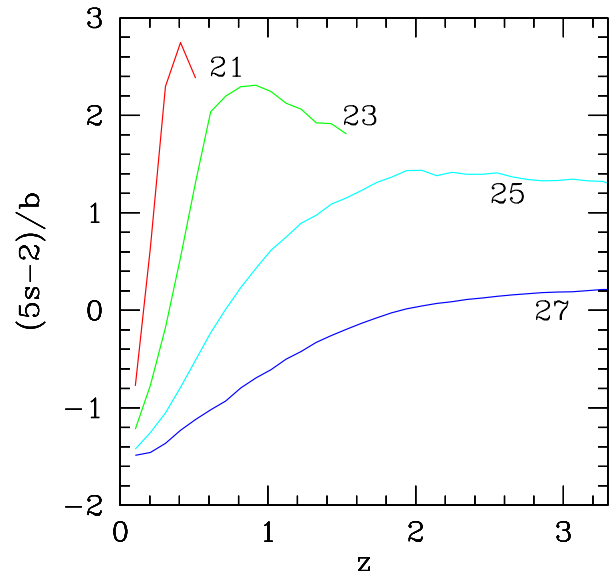


FIG. 1: The ratio $(5s - 2)/b$, where s is the number count slope and b is the galaxy bias, as a function of redshift z for five different galaxy samples. Each sample is defined by a B-band (4344 angstroms) apparent magnitude cut-off as shown for each curve. The curves should be viewed as illustrative rather than definitive: only linear galaxy bias is accounted for here, and the precise values for s and b depend on how the galaxies/quasars are selected e.g. subject to color cuts and so on.

A. The Anisotropic Correlation Function

The observed two-point correlation function is:

$$\begin{aligned} \xi_{\text{obs}}(\chi_1, \boldsymbol{\theta}_1; \chi_2, \boldsymbol{\theta}_2) &= \langle \delta_{\text{obs}}(\chi_1, \boldsymbol{\theta}_1) \delta_{\text{obs}}(\chi_2, \boldsymbol{\theta}_2) \rangle \quad (7) \\ &= \xi_{gg}(\chi_1, \boldsymbol{\theta}_1; \chi_2, \boldsymbol{\theta}_2) + \xi_{g\mu}(\chi_1, \boldsymbol{\theta}_1; \chi_2, \boldsymbol{\theta}_2) \\ &\quad + \xi_{g\mu}(\chi_2, \boldsymbol{\theta}_2; \chi_1, \boldsymbol{\theta}_1) + \xi_{\mu\mu}(\chi_1, \boldsymbol{\theta}_1; \chi_2, \boldsymbol{\theta}_2) \end{aligned}$$

where

$$\begin{aligned} \xi_{gg}(1; 2) &= \langle \delta_g(1) \delta_g(2) \rangle \quad , \quad \xi_{g\mu}(1; 2) = \langle \delta_g(1) \delta_\mu(2) \rangle \quad (8) \\ \xi_{g\mu}(2; 1) &= \langle \delta_g(2) \delta_\mu(1) \rangle \quad , \quad \xi_{\mu\mu}(1; 2) = \langle \delta_\mu(1) \delta_\mu(2) \rangle \end{aligned}$$

with the arguments 1 and 2 as shorthands for $\chi_1, \boldsymbol{\theta}_1$ and $\chi_2, \boldsymbol{\theta}_2$.

Using the Limber approximation, the galaxy-magnification cross-term(s) can be written as:

$$\begin{aligned} \xi_{g\mu}(\chi_1, \boldsymbol{\theta}_1; \chi_2, \boldsymbol{\theta}_2) &= \frac{3}{2} H_0^2 \Omega_m (5s - 2) \quad (9) \\ &\quad (1 + z_1) \frac{(\chi_2 - \chi_1) \chi_1}{\chi_2} \Theta(\chi_1 < \chi_2) \\ &\quad \int \frac{d^2 k_\perp}{(2\pi)^2} P_{gm}(z_1, k_\perp) e^{i\mathbf{k}_\perp \cdot \chi_1 (\boldsymbol{\theta}_1 - \boldsymbol{\theta}_2)} \end{aligned}$$

where $\Theta(\chi_1 < \chi_2)$ is a step function which equals 1 if $\chi_1 < \chi_2$ and vanishes otherwise, H_0 is the Hubble constant today, Ω_m is the matter density today (normalized by the critical density), z_1 is the redshift corresponding to the comoving distance χ_1 , and P_{gm} is the (3D) galaxy-mass power spectrum, and \mathbf{k}_\perp is the transverse Fourier wave vector. We have used the Poisson equation to relate the gravitational potential ϕ to the mass overdensity δ :

$$\nabla^2 \phi = 3H_0^2 \Omega_m (1+z) \delta / 2 \quad (10)$$

Note that the speed of light is set to 1 throughout.

The magnification-magnification correlation, or magnification auto-correlation, is

$$\xi_{\mu\mu}(\chi_1, \boldsymbol{\theta}_1; \chi_2, \boldsymbol{\theta}_2) = \left[\frac{3}{2} H_0^2 \Omega_m (5s - 2) \right]^2 \quad (11)$$

$$\int_0^{\min(\chi_1, \chi_2)} d\chi' \frac{(\chi_1 - \chi')\chi'}{\chi_1} \frac{(\chi_2 - \chi')\chi'}{\chi_2}$$

$$(1 + z')^2 \int \frac{d^2 k_\perp}{(2\pi)^2} P_{mm}(z', k_\perp) e^{i\mathbf{k}_\perp \cdot \chi'(\boldsymbol{\theta}_1 - \boldsymbol{\theta}_2)}$$

where P_{mm} is the (3D) mass-mass power spectrum: it is evaluated at the redshift z' which corresponds to the integration variable χ' .

The focus in the literature has been on ξ_{obs} as an angular correlation: χ_1 and χ_2 are typically integrated over some radial selection functions, and they can signify either two different redshift bins (i.e. angular cross-correlation between galaxies/quasars at two different redshifts [6]), or the same redshift bin (i.e. angular auto-correlation function [4]).

Here, let us take a slightly different perspective: think of ξ_{obs} as a 3D correlation function [13]. For a galaxy survey with redshift information (either spectroscopic redshifts or high quality photometric redshifts), this would be a very natural thing to do. Further, suppose one has a galaxy survey, or a subsample thereof, that spans some finite redshift range such that the radial separation $\chi_1 - \chi_2$ is always small compared to χ_1 or χ_2 . This is a sensible assumption since at sufficiently large separations, galaxy evolution becomes important and complicates one's analysis. Let $\bar{\chi}$ be the mean radial comoving distance to these galaxies, and \bar{z} be the associated mean redshift. The galaxy-magnification cross-correlation and the magnification auto-correlation can be simplified as follows:

$$\xi_{g\mu}(\chi_1, \boldsymbol{\theta}_1; \chi_2, \boldsymbol{\theta}_2) + \xi_{g\mu}(\chi_2, \boldsymbol{\theta}_2; \chi_1, \boldsymbol{\theta}_1) = \quad (12)$$

$$\frac{3}{2} H_0^2 \Omega_m (5s - 2) (1 + \bar{z}) |\chi_2 - \chi_1|$$

$$\int \frac{d^2 k_\perp}{(2\pi)^2} P_{gm}(\bar{z}, k_\perp) e^{i\mathbf{k}_\perp \cdot \bar{\chi}(\boldsymbol{\theta}_1 - \boldsymbol{\theta}_2)}$$

$$\xi_{\mu\mu}(\chi_1, \boldsymbol{\theta}_1; \chi_2, \boldsymbol{\theta}_2) = \left[\frac{3}{2} H_0^2 \Omega_m (5s - 2) \right]^2 \quad (13)$$

$$\int_0^{\bar{\chi}} d\chi' \left[\frac{(\bar{\chi} - \chi')\chi'}{\bar{\chi}} \right]^2 (1 + z')^2$$

$$\int \frac{d^2 k_\perp}{(2\pi)^2} P_{mm}(z', k_\perp) e^{i\mathbf{k}_\perp \cdot \chi'(\boldsymbol{\theta}_1 - \boldsymbol{\theta}_2)}$$

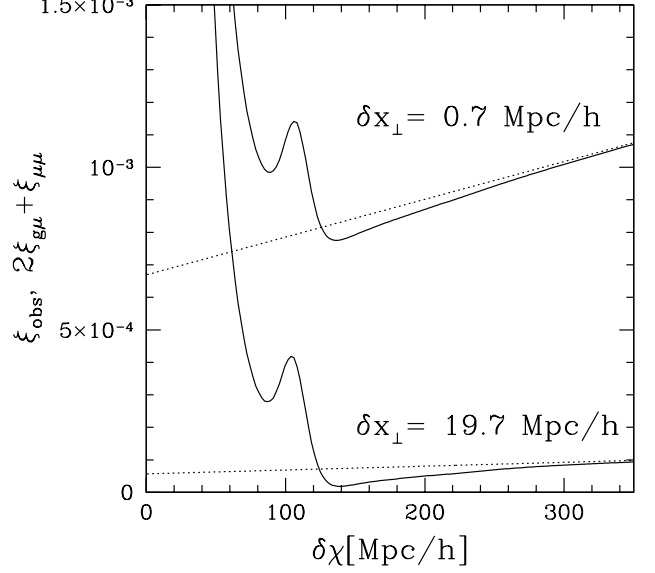


FIG. 2: An illustration of how ξ_{gg} , $\xi_{g\mu}$ and $\xi_{\mu\mu}$ in principle can be obtained from the observed ξ_{obs} . At a given transverse separation δx_\perp (2 examples are shown), ξ_{obs} (solid line) at a large LOS separation $\delta\chi$ is dominated by the magnification corrections $2\xi_{g\mu} + \xi_{\mu\mu}$ which have the form $f(\delta x_\perp)\delta\chi + g(\delta x_\perp)$ i.e. it is linear in $\delta\chi$ (dotted line). The extrapolation of this dotted line to $\delta\chi = 0$ gives g or equivalently $\xi_{\mu\mu}$. Its slope gives f which can be multiplied by $\delta\chi$ to obtain $2\xi_{g\mu}$. Finally, subtracting the dotted line from ξ_{obs} yields ξ_{gg} .

where we have Taylor expanded χ_1 and χ_2 around $\bar{\chi}$ and retained the lowest order contributions. It is useful to compare these two expressions to the intrinsic (unlensed) galaxy auto-correlation, or galaxy-galaxy correlation:

$$\xi_{gg}(\chi_1, \boldsymbol{\theta}_1; \chi_2, \boldsymbol{\theta}_2) = \quad (14)$$

$$\xi_{gg}(\sqrt{(\chi_1 - \chi_2)^2 + \bar{\chi}^2(\boldsymbol{\theta}_1 - \boldsymbol{\theta}_2)^2}) =$$

$$\int \frac{d^3 k}{(2\pi)^3} P_{gg}(\bar{z}, k) e^{i\mathbf{k} \cdot (\mathbf{x}_1 - \mathbf{x}_2)}$$

ignoring for now the issue of redshift distortion, which will be addressed in Paper II. Note that \mathbf{x}_1 and \mathbf{x}_2 refer to the points corresponding to $\chi_1, \boldsymbol{\theta}_1$ and $\chi_2, \boldsymbol{\theta}_2$.

The observed correlation function is a sum of all three correlations above (eq. [7], [12], [13] and [14]). (A discussion of higher order corrections to the latter three can be found in Appendix B.) Viewed in this way, the anisotropy of the lensing induced corrections is quite striking: $\xi_{g\mu}(1, 2) + \xi_{g\mu}(2, 1)$ scales linearly with the line-of-sight (LOS) separation $|\chi_2 - \chi_1|$ (i.e. it increases rather than decreases with the separation!), and $\xi_{\mu\mu}$ is independent of the LOS separation. The intrinsic galaxy auto-correlation ξ_{gg} is isotropic and generally decreases with separation.

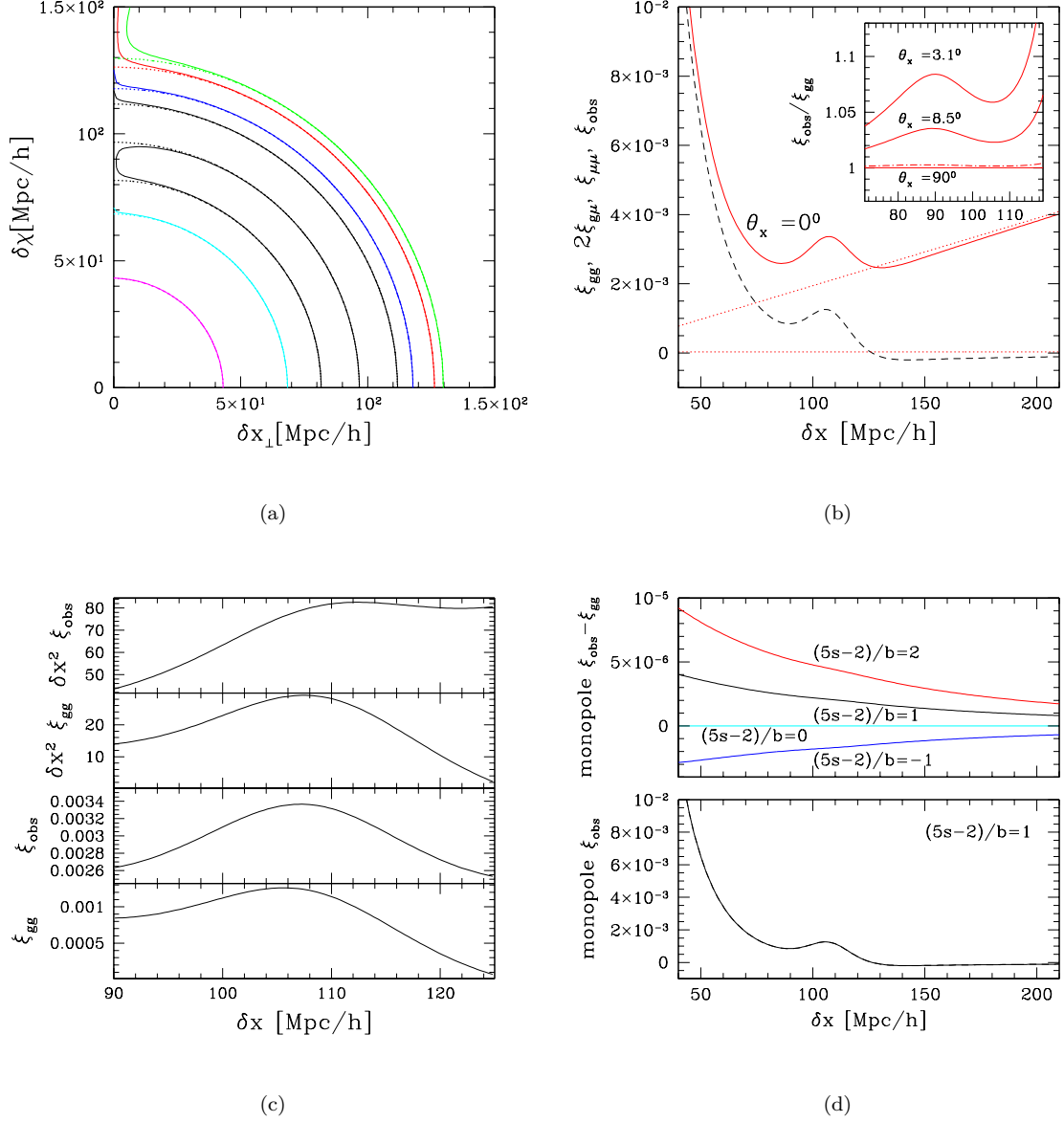


FIG. 3: $\bar{z} = 0.35$: (a) Contours of constant ξ_{obs} (solid) and ξ_{gg} (dotted), left to right: 0.01 (magenta), 0.002 (cyan), 0.001 (black; triple contours), 0.0005 (blue), 0 (red), -0.0001 (green). The LOS separation is $\delta\chi$; the transverse separation is δx_{\perp} . ξ_{gg} is isotropic but ξ_{obs} is not. (b) ξ_{gg} (black dashed), $2\xi_{g\mu}$ (sloped red dotted), $\xi_{\mu\mu}$ (flat red dotted) and ξ_{obs} (red solid) for a separation vector oriented along the LOS. The inset shows the ratio $\xi_{\text{obs}}/\xi_{gg}$ for several other orientations (solid); dot-dashed line shows the ratio of the respective monopoles. Note $\delta x^2 = \delta\chi^2 + \delta x_{\perp}^2$. (c) A zoomed in view of ξ_{gg} , ξ_{obs} , $\delta x^2 \xi_{gg}$, $\delta x^2 \xi_{\text{obs}}$ around the baryon wiggle for a separation vector oriented along the LOS. Note how dangerous it is to use $\delta x^2 \xi_{\text{obs}}$ to locate the baryon peak. (d) Lower panel shows the monopole of ξ_{obs} ; upper panel shows the difference monopole $\xi_{\text{obs}} - \xi_{gg}$ for several different values of $(5s-2)/b$. Unless otherwise stated (as in panel d), $(5s-2)/b = 1$ throughout. All ξ 's are normalized by b^2 .

We can summarize the distinctive lensing induced anisotropy to the observed correlation as follows:

$$\xi_{\text{obs}}(\delta\chi, \delta x_{\perp}) = \xi_{gg}(\sqrt{\delta\chi^2 + \delta x_{\perp}^2}) + f(\delta x_{\perp})\delta\chi + g(\delta x_{\perp}) \quad (15)$$

where $\delta\chi$ and δx_{\perp} are the LOS and transverse separations respectively, $f\delta\chi$ represents the galaxy-

magnification correlation and g represents the magnification-magnification correlation. Here, f and g are functions of the transverse separation only, and are determined by the galaxy-mass and mass-mass power spectra. *This distinctive form of the anisotropy allows us in principle to separately measure ξ_{gg} , f and g , from which we can infer the galaxy-galaxy, galaxy-mass and mass-mass power spectra.* For instance, at any given

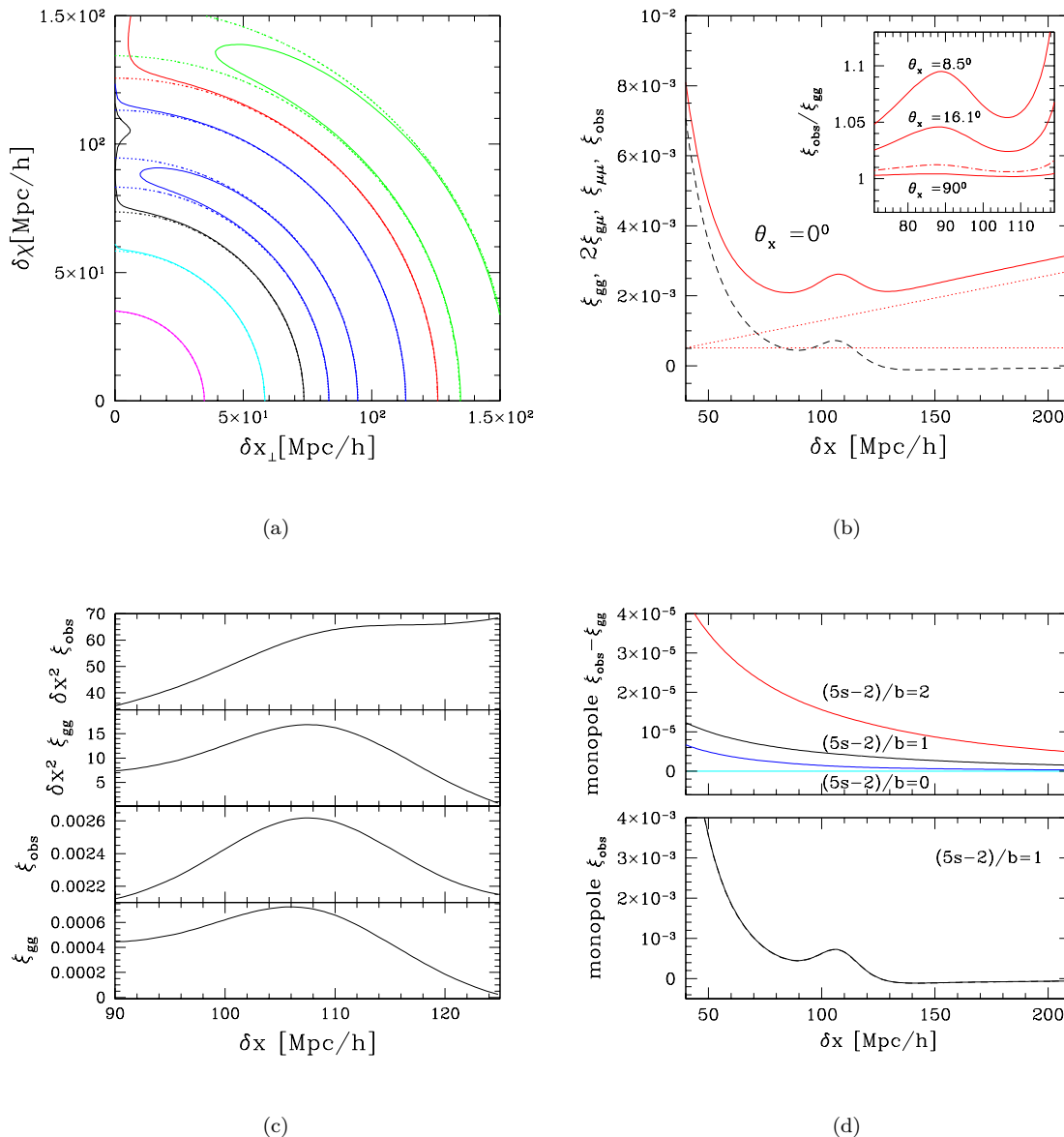


FIG. 4: Analog of Fig. 3 for $\bar{z} = 1$. The contours in (a) are: 0.01 (magenta), 0.002 (cyan), 0.0008 (black), 0.0005 (blue; triple contours), 0 (red) and -0.001 (green; double contours).

δx_{\perp} , plotting ξ_{obs} as a function of the LOS separation $\delta \chi$ would reveal a linear contribution at sufficiently large $\delta \chi$'s where ξ_{gg} is very small. Its slope tells us f and its extrapolation to $\delta \chi = 0$ tells us g . Subtracting $\delta \chi f + g$ from ξ_{obs} then yields ξ_{gg} . This is illustrated in Fig. 2. Fig. 2 should be viewed as a proof of concept only. The optimal method for extracting ξ_{gg} , $\xi_{gg\mu\mu}$ and $\xi_{\mu\mu\mu\mu}$ from realistic data requires more investigation.

Let us study this distortion of the correlation function by magnification bias in more quantitative detail. Fig. 3 - 7 are a series of figures showing several interesting aspects of the observed and intrinsic correlation functions for galaxies at mean redshifts of $\bar{z} = 0.35, 1, 1.5, 2, 3$. These redshifts are chosen to match roughly current and

future surveys [21]. Here, as is throughout the paper, the correlation functions shown in all figures are implicitly divided by b^2 .

Panels (a) show contours of constant ξ_{gg} (dotted) and ξ_{obs} (solid) as a function of the separation vector $\delta \mathbf{x} = \mathbf{x}_1 - \mathbf{x}_2$. Symmetry dictates that the two point correlations are functions of only the LOS projection $\delta \chi = |\chi_1 - \chi_2|$ (y-axis) and the transverse separation $\delta x_{\perp} = \bar{\chi} |\boldsymbol{\theta}_1 - \boldsymbol{\theta}_2|$ (x-axis). Note how certain values of ξ_{gg} or ξ_{obs} map to multiple contours: this is because the correlation function is not monotonic, both around the baryon wobble and beyond the zero-crossing scale (see panels b). Redshift distortion due to peculiar motion is ignored, and therefore ξ_{gg} is isotropic. The observed cor-

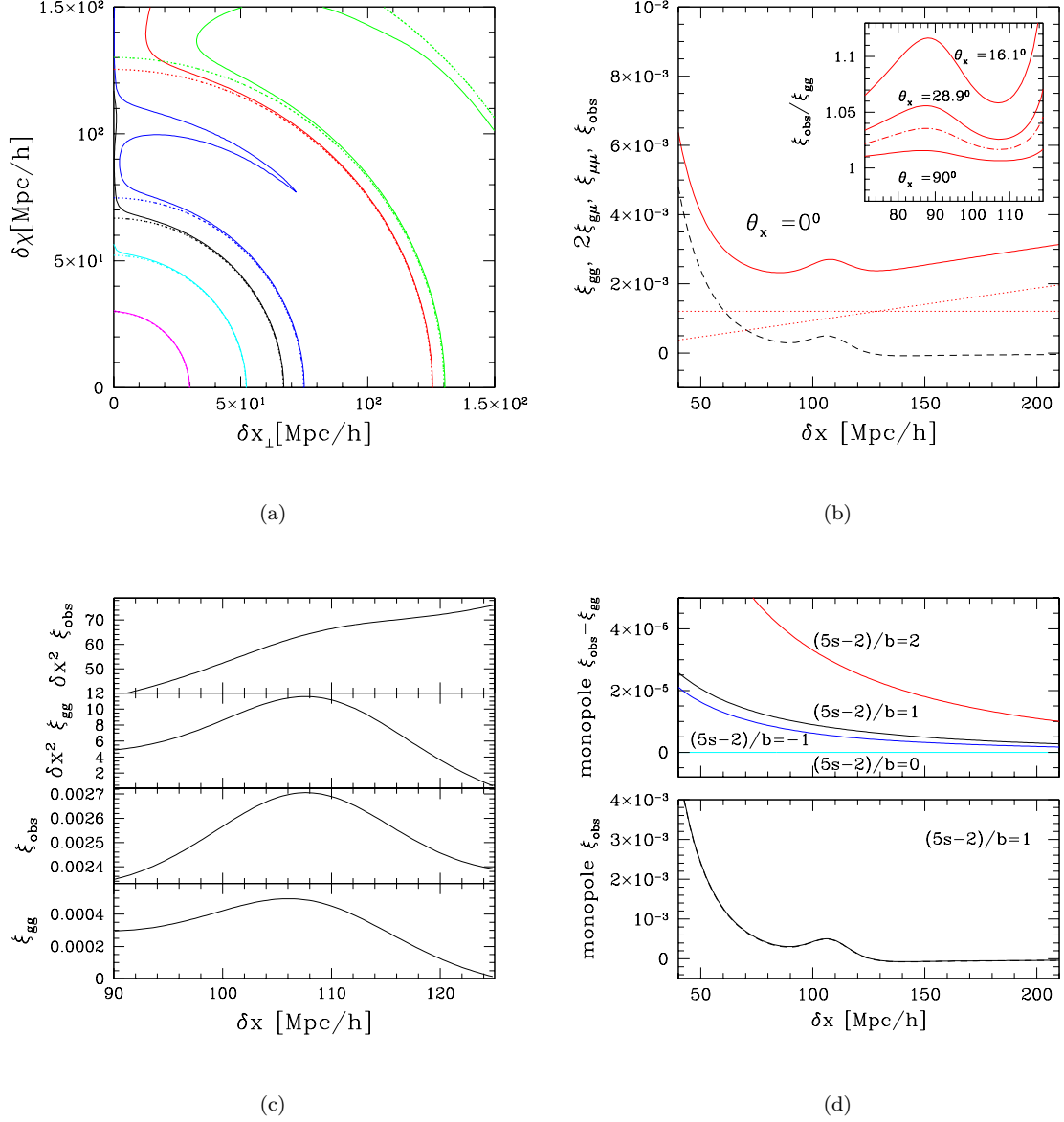


FIG. 5: Analog of Fig. 3 for $\bar{z} = 1.5$. The contours in (a) are: 0.01 (magenta), 0.002 (cyan), 0.0008 (black), 0.0005 (blue), 0 (red) and -0.00005 (green; double contours).

relation ξ_{obs} is anisotropic due to the presence of magnification bias corrections. These corrections are most apparent for pair separations oriented along the LOS. In this orientation, the galaxy-magnification correlation $\xi_{g\mu}$ grows linearly with separation (see eq. [12]) while the intrinsic galaxy-galaxy correlation ξ_{gg} drops with separation. At LOS separations 70 Mpc/h or larger, $\xi_{g\mu}$ dominates over ξ_{gg} . As expected, the magnification distortion of the correlation function becomes increasingly significant at larger redshifts – the distortion is confined to small δx_{\perp} 's at low redshifts, but diffuses to larger δx_{\perp} 's at high redshifts. The overall distortion pattern vaguely resembles the well known finger-of-god (FOG) effect due to virialized motion, in that the contours of constant ξ_{obs}

are elongated in the LOS direction. The precise shapes of the anisotropy, however, are rather different - FOG corrections do not have this linear dependence on the LOS separation that $\xi_{g\mu}$ has. Moreover, FOG due to peculiar motion generally does not extend out to such large scales. We will examine the net clustering anisotropy accounting for both magnification bias and peculiar motion in Paper II. It is also worth emphasizing that $\xi_{g\mu}$ could have the opposite sign if $s < 0.4$, in which case the LOS correlation is enhanced in the negative direction. As can be seen from Fig. 1, unless one has an exceptionally faint magnitude cut-off, s is generally larger than 0.4 at high redshifts where gravitational lensing is most effective.

Panels (b) show ξ_{obs} and its three different contri-

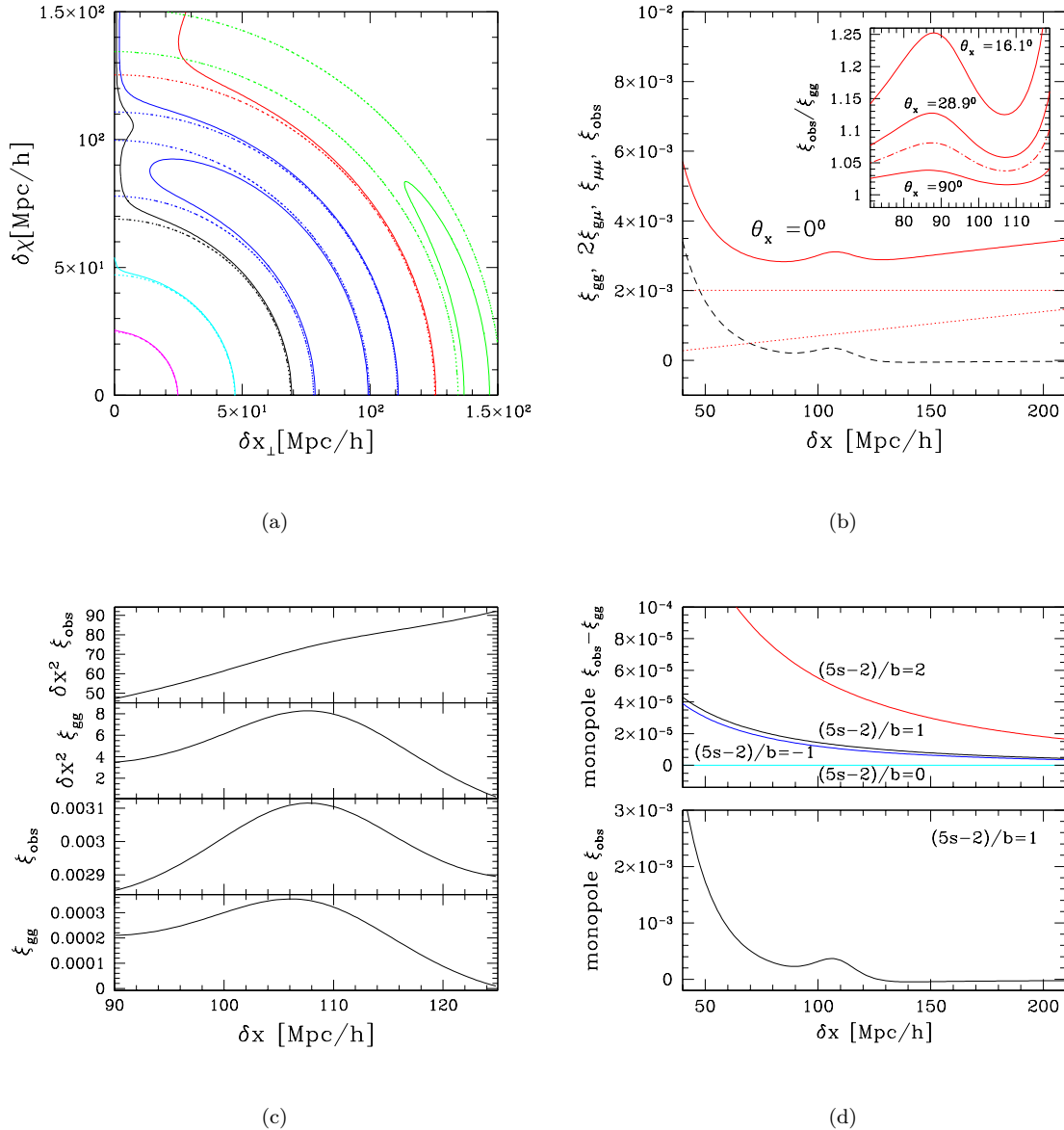


FIG. 6: Analogue of Fig. 3 for $\bar{z} = 2$. The contours in (a) are: 0.01 (magenta), 0.002 (cyan), 0.0005 (black), 0.0003 (blue; triple contours), 0 (red) and -0.00005 (green; double contours).

contributions for a separation vector that is oriented along the LOS ($\theta_x = 0$, where $\cos\theta_x = \delta\chi/\delta x$ with $\delta x = |\delta\mathbf{x}| = \sqrt{\delta\chi^2 + \delta x_\perp^2}$). Eq. (13) tells us $\xi_{\mu\mu}$ (flat dotted line) is independent of the LOS separation, and is therefore simply a constant for this particular orientation. As discussed earlier, $\xi_{g\mu}$ (sloped dotted line) grows linearly with separation in this orientation. The resulting $\xi_{\text{obs}} = \xi_{gg} + 2\xi_{g\mu} + \xi_{\mu\mu}$ is quite a bit larger than ξ_{gg} , even at a redshift as low as $\bar{z} = 0.35$. At a scale of 100 Mpc/h, redshift 1.5 appears to be the transition point between galaxy-magnification dominance and magnification-magnification dominance i.e. $2\xi_{g\mu} \gtrsim \xi_{\mu\mu}$ for $\bar{z} \gtrsim 1.5$, and vice versa. The inset shows the ra-

tio $\xi_{\text{obs}}/\xi_{gg}$ for several other orientations θ_x (solid lines). Comparing the insets for the different redshifts, one can see that at low redshifts this ratio quickly drops to unity as θ_x moves away from zero, while the drop is much less rapid at high redshifts. This is consistent with what we have seen in panel (a): the general diffusion of magnification distortion out to larger values of δx_\perp (and therefore θ_x) as the redshift increases. The dot-dashed line in the inset shows the monopole ξ_{obs} divided by ξ_{gg} . The monopole is defined to be

$$\text{monopole of } \xi_{\text{obs}} = \int_0^{\pi/2} \xi_{\text{obs}}(\delta\mathbf{x}) \sin\theta_x d\theta_x. \quad (16)$$

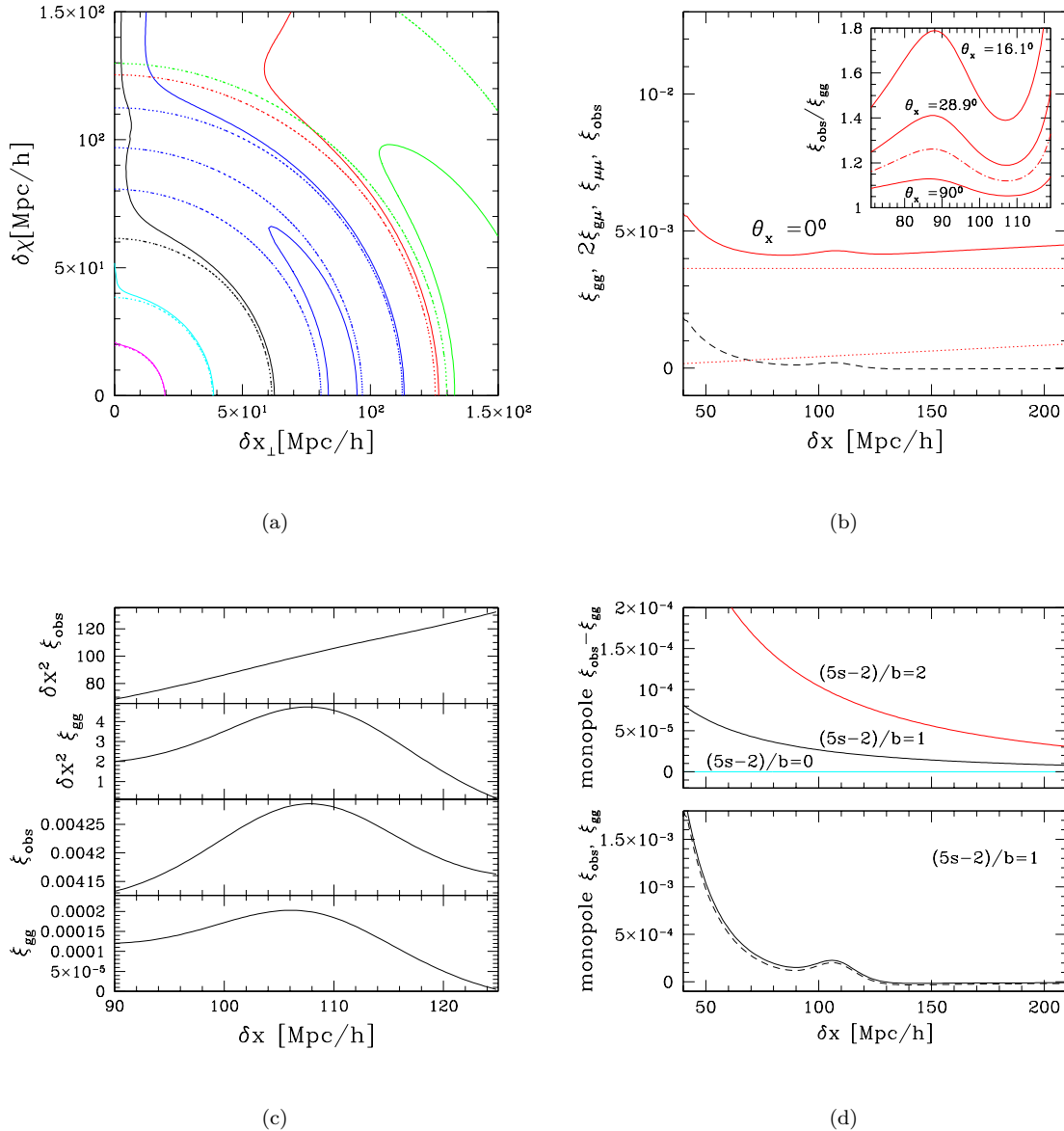


FIG. 7: Analog of Fig. 3 for $\bar{z} = 3$. The contours in (a) are: 0.01 (magenta), 0.002 (cyan), 0.00045 (black), 0.00015 (blue; triple contours), 0 (red) and -0.00002 (green; double contours). The dashed line in the lower panel of (d) is ξ_{gg} .

At a scale of about 100 Mpc/h, the fractional deviation of this monopole from ξ_{gg} is negligible at $\bar{z} = 0.35$, grows to a few percent at $\bar{z} = 1.5$ and is about 20% at $\bar{z} = 3$.

B. Baryon Acoustic Oscillations

Panels (c) of Fig. 3 - 7 zoom in on the baryon wiggle for a separation vector oriented along the LOS. Of interest, probably in descending order, are the location, width and height of the wiggle, and how much they are affected by magnification bias. The answers depend on whether one looks at ξ or, as is commonly done, $\delta x^2 \xi$.

An important lesson here is that $\delta x^2 \xi$ is in fact problematic: in the presence of magnification bias (and for the LOS orientation), the baryon local maximum becomes difficult to locate or disappears completely! Confining ourselves to ξ , the fractional changes in the baryon peak location, width and height induced by magnification bias are shown in the left panel of Fig. 8 for the LOS orientation, and for several different redshifts. Here, we go beyond the assumption of $(5s-2)/b = 1$ in most of the paper, and show these fractional shifts for $(5s-2)/b$ spanning -1 to 2 . The shifts can be quite large. They can have either sign, depending in part on the sign of $5s-2$. The magnitude of the shifts depends sensitively on $(5s-2)/b$ and (for width and height) the redshift. All

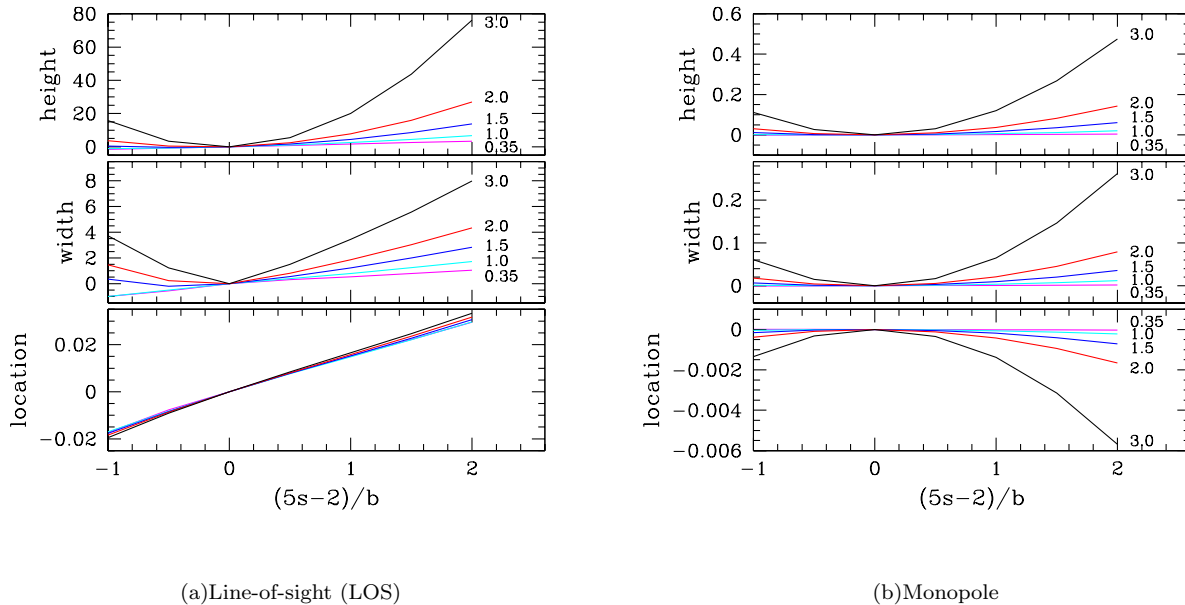


FIG. 8: Fractional shifts in the baryon peak location, width and height as a function of $(5s - 2)/b$ for redshifts spanning 0.35, 1.0, 1.5, 2.0, 3.0. Left panel is for the LOS orientation (where the change in peak location is very similar for different redshifts and the redshift labels are therefore omitted), and right panel is for the monopole. The fractional shift is defined as $(\xi_{\text{obs}} - \xi_{gg})/\xi_{gg}$ for the baryon peak height, and similarly for the peak location and width. The peak width is defined as $[d^2\xi/d\delta x^2/\xi]^{-1/2}$ evaluated at the peak. A note of caution: the precise shifts in these quantities depend on how they are extracted from observations. Panels (d) of Fig. 3 - 7 provide a more complete picture of the effects of magnification bias on the monopole.

the shifts vanish at the special point of $s = 0.4$, where magnification bias is absent. One surprise is that even at a low redshift of 0.35, where one usually expects lensing to be unimportant, the fractional shifts are significant: at $(5s - 2)/b = 1$, they are $\sim 2\%$, $\sim 50\%$ and $\sim 170\%$ for the location, width and height respectively! This is fundamentally because the baryon wiggle is a large scale feature ~ 100 Mpc/h. At such a large separation, the intrinsic galaxy-galaxy clustering is quite weak. The lensing correction, on the other hand, is quite large for the LOS orientation ($\theta_x = 0$) because one galaxy is directly behind another. A location shift of $\sim 2\%$ is significant for baryon oscillation experiments [21]: it corresponds to a $\sim 2\%$ shift in the inferred Hubble parameter $H(z)$, which corresponds to a shift of $\sim 10\%$ for the dark energy equation of state w at the redshifts of interest.

Fig. 8 right panel shows the shifts when one averages over directions i.e. the monopole (eq. [16]). The shifts are much diminished, but in some cases, still non-negligible. For redshifts $\lesssim 1.5$, the location shift is $\lesssim 0.1\%$, but for redshifts $\gtrsim 1.5$, the location shift can reach up to $\sim 0.6\%$. The fractional shifts in width and height are, as before, a bit larger than that in location. An intriguing aspect of Fig. 8 is that, comparing the LOS orientation and the monopole, the location shift actually differs in sign for $(5s - 2)/b > 0$. This suggests that the monopole is dominated by the transverse modes, which

is not surprising, given that the monopole downweights the LOS orientation (eq. [16]).

Note that the monopole can be inferred from data only in a cosmology dependent manner i.e. assumptions need to be made in relating the observed redshift and angular separations to separations in $\delta\chi$ and δx_\perp . Ignoring the anisotropy induced by magnification bias, it can be shown that the baryon peak location in the monopole constrains the combination $(\chi^2/H)^{1/3}$ ([15]; see Appendix in Paper II). A $\sim 0.6\%$ shift in this quantity translates into a $\sim 3\%$ shift in the dark energy equation of state w . One must keep in mind, however, that in the presence of anisotropy, such as that induced by magnification bias, $(\chi^2/H)^{1/3}$ is not the exact quantity that is constrained by the monopole baryon peak. We leave a thorough study of this issue for the future.

One must exercise additional caution in interpreting Fig. 8: the precise shifts in the quantities shown depend on how they are actually extracted from the observational data. Typically, one fits some analytic curve through the data points to locate and characterize the baryon peak. The important point is that magnification bias introduces an additive correction to ξ_{gg} which has a shape that is uncertain: it depends on b , s and the power spectrum. Ignoring this correction leads to errors in one's fit to the data, and therefore biases in the inferred angular diameter distance and Hubble parameter. Precisely

how large a bias one would incur is procedure dependent, and deserves a careful study.

Panels (d) of Fig. 3 - 7 emphasize this point by showing the difference: monopole of $\xi_{\text{obs}} - \xi_{gg}$, for several different values of $(5s - 2)/b$. (We focus on the monopole instead of the LOS orientation, because the monopole is less affected by magnification bias; the difference $\xi_{\text{obs}} - \xi_{gg}$ is quite a bit bigger for the LOS orientation, see panels b of Fig. 3 - 7.) Comparing against the monopole of ξ_{obs} itself, one can see that this difference can be $\sim 10\%$ already by $\bar{z} \sim 1.5$ at the baryon peak. For a limited range of scales around the peak, one can perhaps approximate this difference by some quadratic function, but the precise slope and curvature of this quadratic are uncertain and depend on the galaxy/quasar sample in question. The issue is whether these should be treated as additional parameters in one's fit and how they might affect the accuracy of the peak location measurement. We leave this for a future paper.

III. INTERPRETATION

Fig. 3 - 8 are based on numerically evaluating the integrals in eq. (12), (13) and (14). To gain a deeper understanding of what we have seen, it is useful to develop order of magnitude estimates for the ratios: $\xi_{\mu\mu}/\xi_{gg}$ and $\xi_{g\mu}/\xi_{gg}$.

$$\begin{aligned} \frac{\xi_{\mu\mu}}{\xi_{gg}} &\sim \left[\frac{5s - 2}{b} \right]^2 \frac{(1 + \bar{z})^2}{50} (\bar{\chi} H_0)^3 \frac{\pi H_0}{k_*} \frac{\Delta^2(k_*)}{\Delta^2(k_{**})} \quad (17) \\ \frac{2\xi_{g\mu}}{\xi_{gg}} &\sim \left[\frac{5s - 2}{b} \right] \frac{1 + \bar{z}}{2} (\delta\chi H_0) \frac{\pi H_0}{k_*} \frac{\Delta^2(k_*)}{\Delta^2(k_{**})} \end{aligned}$$

The symbol $\Delta^2(k)$ denotes the dimensionless variance at scale k and redshift \bar{z} : $4\pi k^3 P_{mm}(k)/(2\pi)^3$. Here, $k_{**} \sim 1/\sqrt{\delta\chi^2 + \delta x_\perp^2}$, while k_* is equal to either $1/\delta x_\perp$ or k_m , whichever is smaller (k_m is the scale where $k^2 P_{mm}(k)$ peaks; $k_m \gtrsim 3$ h/Mpc).

The expressions in eq. (17) are only approximate. Among other things, they fail at separations where the correlation functions cross zero or become negative. Away from these separations, we have checked that these expressions reproduce our numerical results quite well, to within factor of a few. Moreover, they make transparent several important points. There are two interesting limits to consider.

One is the limit of a small $\delta\chi$ and a large δx_\perp ($\delta\chi \ll \delta x_\perp$), in which case the factors of Δ^2 's cancel out. It is clear that both correlation ratios should then be small, as long as δx_\perp ($\sim 1/k_*$) is a small fraction of the Hubble scale H_0^{-1} , and the redshift is not too large. A more intuitive way of putting it is that a transverse pair of galaxies (i.e. $\delta\chi = 0$ and $\delta x_\perp \neq 0$) are on average not significantly lensed: for one, they are not lensing each other i.e. the galaxy-magnification term vanishes; as far as the magnification-magnification term is concerned, it

is generally small compared to the intrinsic galaxy correlation unless the redshift is sufficiently high.

The other interesting limit is that of a large $\delta\chi$ and a small δx_\perp ($\delta\chi \gg \delta x_\perp$), in which case $\Delta^2(k_*) \gg \Delta^2(k_{**})$ (because $k_* \sim 1/\delta x_\perp$ and $k_{**} \sim 1/\delta\chi$). This is the limit in which the correlation ratios in eq. (17) can potentially be of order unity or even larger, with the help of the large boost from $\Delta^2(k_*)/\Delta^2(k_{**}) \gg 1$. What is the physical origin of this boost? Consider a pair of galaxies oriented along the LOS (i.e. $\delta\chi \neq 0$ and $\delta x_\perp = 0$). When $\delta\chi$ is large, the intrinsic galaxy correlation is quite weak. The magnification bias corrections, on the other hand, can be relatively large because this is the case of zero lensing impact parameter ($\delta x_\perp = 0$). In other words, one is fundamentally comparing fluctuations on very different scales: large or linear scales in the case of the intrinsic galaxy clustering ξ_{gg} , and small or nonlinear scales in the case of the lensing corrections $\xi_{g\mu}$ and $\xi_{\mu\mu}$. The naive expectation is that one is performing clustering measurements on linear scales by considering pairs of galaxies separated at a large $\delta\chi$ (say 100 Mpc/h), but the truth is that the observed clustering is dominated by nonlinear fluctuations due to lensing.

Incidentally, this also means our linear galaxy bias assumption is probably not a good approximation for pair separations oriented along, or close to, the LOS. The galaxy bias is generally expected to first drop below the linear value for scales just below the nonlinear scale, and then climb when approaching zero lag [11]. This means the effects of gravitational lensing on the LOS orientation should be *enhanced* by a nonlinear galaxy bias compared to our predictions. One can see this by recalling the expression for the observed correlation: $\xi_{\text{obs}} = \xi_{gg} + 2\xi_{g\mu} + \xi_{\mu\mu}$. In the LOS orientation, and for a large separation, the relevant bias for ξ_{gg} is the linear galaxy bias b that we have been using all along, while the relevant bias for $\xi_{g\mu}$ (at $\delta x_\perp = 0$) should really be a nonlinear and presumably enhanced galaxy bias $> b$. Therefore, the effects of gravitational lensing are in fact *underestimated* by our calculations which use a linear galaxy bias. The precise scale dependence though of the nonlinear galaxy bias is quite complicated and is highly sample dependent. We hope to pursue a thorough study of the effects of nonlinear galaxy bias in the future. It is important to stress that the distinctive anisotropy displayed in eq. (15) holds true even in the presence of nonlinear galaxy bias – this is because eq. (15) follows from eq. (12), (13) and (14) which make no assumptions about galaxy biasing.

Irrespective of details of the nonlinear galaxy bias, the following statement is expected to hold: *magnification-bias has the strongest effect on the observed correlation function when the separation $\delta\mathbf{x}$ has a large magnitude and points close to the line-of-sight direction.*

Eq. (17) also tells us that $\xi_{\mu\mu}$ is generally expected to be larger than $\xi_{g\mu}$ when the redshift is sufficiently large. Sufficiently large here means when $\bar{\chi} H_0 \gtrsim 1$. This occurs at $\bar{z} \sim 1.5$ for the cosmological parameters we adopt.

Conversely, $\xi_{\mu\mu}$ is generally quite small at low redshifts because of the cubic power in the factor $(\bar{\chi}H_0)^3$. In this case, $\xi_{g\mu}$ is more favored if the LOS separation $\delta\chi$ is large enough.

IV. DISCUSSION

Our findings can be summarized as an opportunity and a challenge.

Opportunity. Gravitational lensing, through magnification bias, introduces a distinctive anisotropy to the observed 3D galaxy/quasar correlation function (eq. [15]). We have studied its shape in §II A. The correlation is preferentially enhanced (in the positive direction for $s > 0.4$) in the LOS orientation, vaguely resembling the finger-of-god (FOG) effect due to virialized peculiar motions. However, as will be discussed in detail in Paper II, the precise shape of magnification distortion differs from that of FOG or redshift distortion in general – redshift distortion does not have the distinctive linear dependence on the LOS separation that $\xi_{g\mu}$ has. The distinctive lensing induced pattern creates an interesting opportunity: it is in principle possible to separately obtain from data all three contributions: the galaxy-galaxy, galaxy-magnification *and* magnification-magnification correlations (Fig. 2). This generalizes earlier work on magnification bias [6, 7, 8, 9, 10] which focused on angular correlations in the large redshift separation limit, where only the galaxy-magnification correlation survives. Future galaxy/quasar (spectroscopic or photometric) redshift surveys can be used to measure the galaxy-galaxy, galaxy-mass and mass-mass power spectra, even without measurements of the galaxy shapes.

Challenge. The same effect must be accounted for in interpreting galaxy/quasar clustering data. This presents an interesting challenge to precision measurements, such as those that hope to use the baryon oscillation scale to yield stringent constraints on dark energy. Contrary to naive expectations, magnification bias is not necessarily negligible at low redshifts. In the LOS orientation, where its effects are largest, the shift in the baryon oscillation scale is remarkably insensitive to redshifts, from $\bar{z} \sim 0.35$ to $\bar{z} \sim 3$ (Fig. 8 panel a). The shift could reach up to $\sim 2 - 3\%$, which translates to a $\sim 10 - 15\%$ shift in the dark energy equation of state from the inferred Hubble parameter. Existing baryon oscillation measurements [15, 16, 17, 18, 19] have not reached this kind of accuracy, but the future ones will [21]. The shift for other orientations are smaller. We have considered the shift in the monopole and find that it is much diminished, reaching up to $\sim 0.6\%$ at $\bar{z} \sim 3$ (Fig. 8 panel b). However, one should keep in mind that the precise shifts really depend on exactly how the baryon oscillation scale is extracted from data. The point is that magnification bias introduces corrections to the correlation function that are dependent on scale, bias and the number count slope, for all orientations and for the monopole (Fig. 3 - 7 panels d).

The question is when data are fitted without accounting for these corrections, what kind of bias would one incur in the inferred parameters?

This leads us naturally to several interesting questions to be explored in the future.

On the opportunity side, what is the optimal scheme to extract the galaxy-galaxy, galaxy-magnification and magnification-magnification correlations from realistic data? Fig. 2 represents a proof of concept but is likely not the optimal method. How to best weigh the relative contributions of different galaxies with different bias and number count slope? Also, how to best guard against the possibility of confusion with dust extinction? The distinctive dependence of the magnification corrections on the number count slope can probably be exploited for this purpose [8].

On the challenge side, how would magnification bias impact baryon oscillation measurements if one accounts for precisely how the oscillation scale might be extracted from future data? How might the impact be different in Fourier space versus real space? We will address this question partially in Paper II.

Our calculations assumed a constant bias b which is certainly incorrect at some level. A complete calculation that accounts for nonlinear bias and distortions of all types (peculiar motions, Alcock-Paczynski and magnification bias) should be made to properly interpret precision galaxy clustering measurements [29]. Lastly, in light of our findings, it is probably interesting to revisit some longstanding puzzles, such as the well known results of the pencil beam surveys by [30, 31]. The enhancement of the LOS correlation by magnification bias offers a plausible explanation for the excess correlations, though not the periodicity, seen in [30]. With the magnitude cut-off used by [30], it is likely that $(5s - 2)/b \sim 1$ (see also [32]), in which case we can scale the result of Fig. 3(c) to the mean redshift of ~ 0.2 using eq. (17) and obtain an enhancement factor of ~ 2 at the scale ~ 100 Mpc/h. Coupled this with the fact that the baryon wiggle was not taken into consideration back in the days of [30], the total enhancement factor by magnification bias + baryon oscillations is ~ 4 . Moreover, as noted in §III, accounting for nonlinear galaxy bias in the lensing correction would likely lead to a further enhancement factor of a few. The net enhancement factor could well be ~ 10 , making the excess correlations seen in [30] within reach. It would be worthwhile to carry out a more careful analysis, taking into account properties of the precise galaxy sample in question, and the actual widths of the pencil beams. It might also be interesting to revisit some of the measurements of Lyman-break galaxy clustering at $z \sim 3$ [33] in the light of our findings.

Acknowledgments

We thank Roman Scoccimarro and Albert Stebbins for useful discussions. We also thank Taka Matsubara

and Asantha Cooray for pointing out to us an important missing reference in our first preprint. Research for this work is supported by the DOE, grant DE-FG02-92-ER40699, and the Initiatives in Science and Engineering Program at Columbia University. EG acknowledges support from Spanish Ministerio de Ciencia y Tecnología (MEC), project AYA2006-06341 with EC-FEDER funding, and research project 2005SGR00728 from Generalitat de Catalunya.

APPENDIX A: MAGNIFICATION BIAS AND OTHER LENSING CORRECTIONS TO THE OBSERVED GALAXY CLUSTERING

In this Appendix, we attempt to be as general as possible in considering the effect of gravitational lensing on the apparent spatial clustering of galaxies. In the process, we will rederive the magnification bias effect, generalizing it to the case of a gradual rather than sharp magnitude cut-off. We will also discuss the role of stochastic deflections which contribute to higher order corrections.

Let $\Phi_g(f_g, z, \boldsymbol{\theta}_g)df_g$ be the intrinsic number density of galaxies at redshift z , source (unlensed) position $\boldsymbol{\theta}_g$, and an unlensed flux in the range $f_g \pm df_g/2$. We use the subscript g to denote quantities that are intrinsic to the galaxies, or in other words, prelensed/unlensed quantities. Note also that the number density here can refer to either an angular number density or a volume number density. Gravitational lensing introduces the transformations $f_g \rightarrow f$, $\boldsymbol{\theta}_g \rightarrow \boldsymbol{\theta}$ and $\Phi_g \rightarrow \Phi$, which satisfy the following relations:

$$\Phi(f, z, \boldsymbol{\theta})df d^2\theta = \Phi_g(f_g, z, \boldsymbol{\theta}_g)df_g d^2\theta_g \quad (\text{A1})$$

where

$$\begin{aligned} \boldsymbol{\theta}_g &= \boldsymbol{\theta} + \delta\boldsymbol{\theta} \\ f &= Af_g \\ \det. \left[\frac{\partial\theta_g^i}{\partial\theta^j} \right] &\equiv 1/A \end{aligned} \quad (\text{A2})$$

The quantity A denotes the magnification in the observed direction $\boldsymbol{\theta}$, and $\delta\boldsymbol{\theta}$ is the lensing displacement.

A given galaxy sample can be modeled by an efficiency function $\epsilon(f)$ such that the observed galaxy density is

$$n(z, \boldsymbol{\theta}) = \int \epsilon(f)\Phi(f, z, \boldsymbol{\theta})df \quad (\text{A3})$$

The simplest example of $\epsilon(f)$ is a step function which equals unity if $f > f_{\min}$. and vanishes otherwise:

$$\epsilon(f) = \Theta(f_{\min} < f) \quad (\text{A4})$$

but let us keep $\epsilon(f)$ general.

Using eq. (A1) and (A2), we can see that

$$n(z, \boldsymbol{\theta}) = \frac{1}{A(z, \boldsymbol{\theta})} \int \epsilon(Af_g)\Phi_g(f_g, z, \boldsymbol{\theta} + \delta\boldsymbol{\theta})df_g \quad (\text{A5})$$

Note that the lensing magnification A is a function of both the source redshift z and the direction $\boldsymbol{\theta}$.

Our expressions so far are completely general: no weak lensing approximation has been made (aside from not summing over multiple $\delta\boldsymbol{\theta}$'s to account for the possibility of multiple images). One could if one wishes use eq. (A5) as the starting point for investigating the lensed galaxy clustering. The discussion is much simplified, however, under the weak lensing approximation i.e. $A \sim 1 + 2\kappa$, where $|\kappa| \ll 1$. In that case,

$$n(z, \boldsymbol{\theta}) = n_g(z, \boldsymbol{\theta} + \delta\boldsymbol{\theta}) [1 + (5s - 2)\kappa] \quad (\text{A6})$$

where

$$n_g = \int \epsilon(f_g)\Phi_g(f_g)df_g \quad (\text{A7})$$

is the galaxy density if lensing magnification were absent (we have suppressed the z and $\boldsymbol{\theta} + \delta\boldsymbol{\theta}$ dependence), and

$$s \equiv [2.5n_g]^{-1} \int \frac{d\epsilon}{df_g} f_g \Phi_g(f_g)df_g \quad (\text{A8})$$

The definition of s might look a bit unfamiliar, but if ϵ does indeed take the form of the step function (eq. [A4]), s is the (magnitude) slope of the cumulative number counts at the faint end cut-off:

$$s = \frac{d\log_{10}n_g}{dm} \quad (\text{A9})$$

where $m \equiv -2.5\log_{10}f$ and the derivative is evaluated at $m = -2.5\log_{10}f_{\min}$.

As long as $\langle A \rangle = 1$ (or $\langle \kappa \rangle = 0$) which holds if multiple imaging can be ignored, $\langle n \rangle = \langle n_g \rangle$. Let us call this mean density \bar{n} . The fluctuation in the observed galaxy density $\delta \equiv n/\bar{n} - 1$ is related to the fluctuation in the intrinsic galaxy density $\delta_g \equiv n_g/\bar{n} - 1$ by

$$\begin{aligned} \delta(z, \boldsymbol{\theta}) &= \delta_g(z, \boldsymbol{\theta} + \delta\boldsymbol{\theta}) + \\ &(5s - 2)\kappa(z, \boldsymbol{\theta}) \times (1 + \delta_g(z, \boldsymbol{\theta} + \delta\boldsymbol{\theta})) \end{aligned} \quad (\text{A10})$$

This is equivalent to eq. (2) and (3) used in the rest of the paper, except that we have consistently ignored the effects of stochastic deflection $\delta\boldsymbol{\theta}$, and we have consistently neglected $\kappa\delta_g$ as small. In other words, gravitational lensing strictly speaking should have 2 qualitatively different effects on the observed galaxy clustering. Magnification bias is embodied in the term $(5s - 2)\kappa$, which accounts for the effect of an overall magnification (or demagnification) on the number counts. Stochastic deflections, on the other hand, introduces a remapping of the galaxy density field. The remapped field can be Taylor expanded as

$$\delta_g(\boldsymbol{\theta} + \delta\boldsymbol{\theta}) \sim \delta_g(\boldsymbol{\theta}) + \sum_i \frac{\partial\delta_g}{\partial\theta^i} \delta\theta_i \quad (\text{A11})$$

The approximation we have been making is in effect a linear approximation: the second term on the right is

second order in perturbations and is therefore ignored (just as we throw away the $\kappa\delta_g$ term also). Similarly, the s defined in eq. (A8) can be replaced by one with $f_g \rightarrow f$ and $\Phi_g \rightarrow \Phi$. Corrections to this when multiplied by κ as in eq. (A10) are second order.

It is worth emphasizing that the gravitational lensing effect on diffuse backgrounds, such as the microwave background or redshifted 21cm background, is quite different [34, 35]. There, because the observable is specific intensity which is conserved by lensing, the *only* lensing effect is remapping by stochastic deflections i.e. there is no analog of the magnification bias term $(5s - 2)\kappa$.

One might worry that in the nonlinear regime where δ_g is not small, one should not ignore the effects of stochastic deflection relative to magnification bias. This certainly deserves more study. Zahn & Zaldarriaga [35] carried out a detailed study of the impact of stochastic deflection on the redshifted 21cm background, including all higher order terms. Stochastic deflection appears to have a rather small overall impact, suggesting that ignoring it might not be a bad approximation.

APPENDIX B: HIGHER ORDER CORRECTIONS

Eq. (12), (13) and (14), and the corresponding expressions in Fourier space, are written down by keeping only the dominant terms in an expansion using $(\chi_1 - \bar{\chi})/\bar{\chi}$ or $(\chi_2 - \bar{\chi})/\bar{\chi}$ as a small parameter. It is worth discussing how large the corrections are expected to be. One might naively expect the corrections to be one order higher: for instance, that the dominant correction to $\xi_{\mu\mu}(1; 2)$ should be of the order of what is given in eq. (13) multiplied by $(\chi_1 - \chi_2)/\bar{\chi}$. This expectation turns out to be false for

$\xi_{\mu\mu}$ and ξ_{gg} , but valid for $\xi_{g\mu}$. Let us see how this comes about in the case of $\xi_{\mu\mu}$. Taylor expanding eq. (11) for $\xi_{\mu\mu}(1; 2)$ in small $\delta\chi_1 = \chi_1 - \bar{\chi}$ and $\delta\chi_2 = \chi_2 - \bar{\chi}$, we have

$$\xi_{\mu\mu}(\chi_1, \boldsymbol{\theta}_1; \chi_2, \boldsymbol{\theta}_2) = \left[\frac{3}{2}H_0^2\Omega_m(5s - 2)\right]^2 \quad (\text{B1})$$

$$\int_0^{\bar{\chi}} d\chi' \left[\frac{(\bar{\chi} - \chi')\chi'}{\bar{\chi}}\right]^2 (1 + z')^2$$

$$\int \frac{d^2k_\perp}{(2\pi)^2} P_{mm}(z', k_\perp) e^{i\mathbf{k}_\perp \cdot \chi'(\boldsymbol{\theta}_1 - \boldsymbol{\theta}_2)}$$

$$[1 + O(\delta\chi_1/\bar{\chi}) + O(\delta\chi_2/\bar{\chi})]$$

where the terms $O(\delta\chi_1/\bar{\chi})$ and $O(\delta\chi_2/\bar{\chi})$ signify all the next-to-dominant order corrections which in general do not vanish. The important realization is that the term $O(\delta\chi_1/\bar{\chi})$ and the term $O(\delta\chi_2/\bar{\chi})$ have exactly the same coefficients, and so they sum to zero as long as $\delta\chi_1 + \delta\chi_2 = 0$ i.e. $\bar{\chi}$ is the mean of χ_1 and χ_2 . Therefore, one has to go one order higher in the Taylor expansion to figure out the actual corrections. A similar argument works for the galaxy auto-correlation ξ_{gg} . The magnification-galaxy cross-correlation $\xi_{g\mu}(1; 2) + \xi_{g\mu}(2; 1)$, on the other hand, turns out to be different: in this case, the analogous terms $O(\delta\chi_1/\bar{\chi})$ and $O(\delta\chi_2/\bar{\chi})$ have different coefficients. In general, when the pair (1; 2) is averaged over some survey volume, one expects the (fractional) correction to our expression for the magnification-galaxy cross-correlation to be $O(|\chi_1 - \chi_2|/\bar{\chi})$. If one is worried about this correction, there is no reason why one cannot use instead the exact expression (within Limber approximation) for $\xi_{g\mu}$ in eq. (9).

-
- [1] E. L. Turner, J. P. Ostriker, J. R. Gott, *Astrophys. J.* 284, 1 (1984); R. L. Webster, P. C. Hewett, M. E. Harding, G. A. Wegner, *Nature* 336, 358 (1988); W. Fugmann, *Astron. & Astrophys.* 204, 73 (1988); R. Narayan, *Astrophys. J. Lett.* 339, 53 (1989); P. Schneider, *Astron. & Astrophys.* 221, 221 (1989).
 - [2] J. Villumsen, preprint (1995) [astro-ph/9512001].
 - [3] J. Villumsen, W. Freudling, L. N. da Costa, *Astrophys. J.* 481, 578 (1997).
 - [4] R. Moessner, B. Jain, J. Villumsen, *Mon. Not. R. Astron. Soc.* 294, 291 (1998)
 - [5] N. Kaiser, *Astrophys. J.* 498, 26 (1998)
 - [6] R. Moessner, B. Jain, *Mon. Not. R. Astron. Soc.* 294, L18 (1998).
 - [7] E. Gaztañaga, *Astrophys. J.* 589, 82 (2003).
 - [8] R. Scranton, et al., *Astrophys. J.* 633, 589 (2005).
 - [9] B. Menard, . Bartelmann, *Astron. & Astrophys.* 386, 784 (2002).
 - [10] B. Jain, *Astrophys. J. Lett.* 580, 3 (2002).
 - [11] B. Jain, R. Scranton, R. K. Sheth, *Mon. Not. R. Astron. Soc.* 345, 62 (2003).
 - [12] T. J. Broadhurst, A. N. Taylor, J. A. Peacock, *Astrophys. J.* 438, 49 (1996).
 - [13] T. Matsubara, *Astrophys. J. Lett.* 537, 77 (2000).
 - [14] L. Hui, E. Gaztañaga, M. LoVerde, submitted to *Phys. Rev. D*, (2007) [Paper II].
 - [15] D. J. Eisenstein et al., *Astrophys. J.* 633, 560 (2005)
 - [16] S. Cole et al., *Mon. Not. R. Astron. Soc.* 362, 505 (2005)
 - [17] W. J. Percival et al., preprint (2006) [astro-ph/0608635]
 - [18] G. Hütsi, *Astron. & Astrophys.* 449, 891 (2006)
 - [19] M. Tegmark et al., preprint (2006) [astro-ph/0608632]
 - [20] An incomplete list of theoretical papers on the use of baryon oscillations to measure dark energy includes: C. Blake, K. Glazebrook, *Astrophys. J.* 594, 665 (2003); E. Linder, *Phys. Rev. D* 68, 082504 (2003); W. Hu, Z. Haiman, *Phys. Rev. D* 68, 063004 (2003); J. J. Seo, D. J. Eisenstein, *Astrophys. J.* 598, 720 (2003); A. Cooray, *Mon. Not. R. Astron. Soc.* 348, 250 (2004); T. Matsubara, *Astrophys. J.* 615, 573 (2004); L. Amendola, C. Quercellini, & E. Giallongo, *Mon. Not. R. Astron. Soc.* 357, 429 (2005); C. Blake & S. Bridle, *Mon. Not. R. Astron. Soc.* 363, 1329 (2005).
 - [21] An incomplete list of planned/proposed surveys to measure the baryon acoustic oscillations includes: ADEPT

- (http://www.jhu.edu/news_info/news/home06/aug06/adept.html), DES Dark Energy Survey (Annis et al., from <http://decam.fnal.gov>, <http://www.darkenergysurvey.org>), FMOS/WFMOS at Gemini/Subaru [astro-ph/0507457], HETDEX (<http://www.as.utexas.edu/hetdex>), WiggleZ (<http://astronomy.swin.edu.au/~karl/Karl-Home/Home.html>).
- [22] M. LoVerde, L. Hui, E. Gaztañaga, submitted to Phys. Rev. D, (2007).
- [23] A. Vallinotto, S. Dodelson, C. Schmid, J.-P. Uzan (2007) [astro-ph/0702606].
- [24] C. Wagner, V. Muller, M. Steinmetz, preprint (2007) [arXiv:0705.0354]
- [25] A. Gabasch et al., Astron. & Astrophys. 421, 41 (2004) [astro-ph/0403535]; A. Gabasch et al., Astron. & Astrophys. in press (2006) [astro-ph/0510339]. To be precise: we make use of Table 4 of the former, and Table 9 (Case 3) of the latter, and linearly interpolate between adjacent rest bands.
- [26] M. LoVerde, L. Hui, E. Gaztañaga, Phys. Rev. D 75, 043519 (2007) [astro-ph/0611539]
- [27] D. J. Eisenstein, W. Hu, Astrophys. J. 496, 605 (1998)
- [28] R. E. Smith et al., Mon. Not. R. Astron. Soc. 341, 1311 (2003)
- [29] There are many recent papers on how nonlinearity, nonlinear bias and redshift distortion affect the baryon oscillations in the 3D correlation function: see T. Nishimichi et al., preprint (2007) [arXiv:0705.1589] and references therein. None of these included magnification bias, however.
- [30] T. J. Broadhurst, R. S. Ellis, D. C. Koo, A. S. Szalay, Nature 343, 726 (1990)
- [31] A. Szalay, T. J. Broadhurst, N. Ellman, D. C. Koo, R. S. Ellis, Proc. Natl. Acad. Sci. 90, 4853 (1993)
- [32] N. Metcalfe, T. Shanks, R. Fong, N. Roche, Mon. Not. R. Astron. Soc. 273, 257 (1995)
- [33] K. L. Adelberger et al., Astrophys. J. 505, 18 (1998); K. L. Adelberger et al., Astrophys. J. 619, 697 (2005)
- [34] U. Seljak, Astrophys. J. 463, 1 (1996); M. Zaldarriaga, U. Seljak, Phys. Rev. D 58, 023003 (1998); A. Cooray, New Astronomy 9, 173 (2004); B. Metcalf, S. D. M. White, preprint (2006) [astro-ph/0611862]
- [35] O. Zahn, M. Zaldarriaga, Astrophys. J. 653, 922 (2006)